Accepted manuscript (author version)

To appear in:

Iranian Journal of Earth Sciences (Iran J. Earth. Sci.)

E-ISSN: 2228-785X Print ISSN: 2008-8779

Received: 1 March 2025

Revised: 19 April 2025

Accepted: 9 June 2025

DOI: https://doi.org/10.57647/j.ijes.2025.17560

Original Research

Comprehensive analysis of gastropod species in the loess-paleosol sequence of Sa'dabad-3, Gorgan, Iran

Fatemeh Fadavi[1], Mehry Akbari[1], Elham Ahmadi[2]*, Farhad Khormali[3], Sahar Maleki[4]

[1] Department of Natural Geography Faculty of Geographical Sciences, Kharazmi University, Tehran, Iran

[2] Agricultural Zoology Research Department, Iranian Research Institute of Plant Protection, Agricultural Research, Education and Extension Organization (AREEO), Tehran, Iran

[3] Department of Soil Science, Gorgan University of Agricultural Sciences and Natural Resources, Gorgan, Iran

[4]Geological Survey of Iran, Tehran, Iran

* Corresponding author: e1_ahmadi@yahoo.com

Abstract

Through the examination of land snail shells embedded in the loess-paleosol succession of Sa'dabad-3, this research provides a valuable perspective on past environmental changes and contributes to a better understanding of Quaternary climatic fluctuations in northern Iran. A total of 12,910 mollusk shell specimens were collected from 230 samples taken at 10 cm intervals along the 23-meter-thick Sa'dabad-3 loess–paleosol section, and identified to species level via morphological examination. Although no direct geochronology was performed, the undated Sa'dabad-3 sequence was correlated with dated loess-paleosol sections at Now Deh and Agh Band to establish an approximate chronological framework. In total, 37 land snail species were identified, 16 of which are newly recorded for Golestan Province. Seven malacological zones were distinguished based on stratigraphic variations in mollusk abundance and diversity, reflecting alternating glacial (loess deposition) and interglacial (paleosol formation) intervals. Paleosol layers generally yielded richer assemblages, with a higher proportion of hygrophilous (moisture-loving) species, indicative of relatively warm, humid climates, whereas loess layers mostly contained fewer shells and reflect colder, drier conditions. However, a few exceptions to this pattern were observed, likely due to local taphonomic or microenvironmental factors. By correlation with regional loess records, the Sa'dabad-3 succession is inferred to span from Marine Isotope Stage 7 (~250–300 ka). The Sa'dabad-3 land snail shell assemblages represent valuable proxies for Quaternary climate reconstruction in northern Iran. These findings demonstrate the effectiveness of land snails as paleoenvironmental indicators and underscore the importance of integrating malacological data into multi-proxy climate studies.

Keyword: Quaternary, Land snails, loess, paleoclimate, paleoenvironment.

1. Introduction

Paleoclimatology studies reveal that Earth's climate is continuously changing. Climatic fluctuations such as droughts, floods, and storms have always impacted human life. Examining past climate variations and analyzing them over time allows for the identification of specific patterns. These patterns can be instrumental in enhancing management strategies and predicting future climatic changes. Many climatic studies conducted in Iran have focused on short-term periods, typically between 20 to 50 years. The existing data on past climatic changes, mainly pertaining to the last 150 years and derived from satellites and meteorological stations, have limitations. These constraints make it difficult or even impossible to identify climate change patterns over longer periods, especially beyond this timeframe. Additionally, due to the relatively short lifespan of meteorological stations in the country, their uneven distribution, the scarcity of synoptic stations, and the focus of most studies on temperature averages, the credibility and accuracy of these short-term studies have diminished. Understanding climatic patterns over extended periods can significantly aid in identifying future climate changes and making informed management decisions. Therefore, a precise examination of past climatic changes using valid climatological indicators has become highly important. This has highlighted the importance of using sedimentary archives for paleoclimate reconstruction. In this context, geochemical studies on core sediments from the southern coast of the Caspian Sea have shown that these sediments reflect semi-arid to arid paleoclimatic conditions and can play a significant role in climate reconstruction (Chenari et al., 2025). One of the major challenges in this field is the lack of climatic data in terrestrial sediments, which hinders the precise correlation between these sediments and Marine Isotope Stages (MIS) (Rutter et al., 2003).

The accumulation of loess deposits is one of the most significant consequences of climate changes during the Quaternary period and is recognized as the most comprehensive terrestrial archive of Quaternary climate. Loess is a clastic sediment with silt-sized particles, primarily composed of wind-blown dust; it is porous and lacks stratification. Loess deposits cover about 10% of Earth's surface during the Quaternary period. This geological era is climatically significant due to its regular climatic cycles, including glacial and interglacial periods. During glacial periods, loess deposits form, and during interglacial periods, paleosols develop (Liu, Ding, & Rutter, 1999). Research on loess in Iran has gained considerable attention since the beginning of the 21st century. Northern Iran, particularly Golestan Province, is recognized as a key area in this field. It connects Europe and Asia and contributes to completing the paleoclimate puzzle along the loess belt that extends from Eastern Europe to Central Asia and China (Ghafarpour et al., 2016; Vlaminck et al., 2018). Investigating the loess-paleosol sequences in this region is especially important due to their unique geographical location and significant thicknesses, reaching up to 30 meters on the slopes of the Alborz Mountain range and about 60 meters on the loess plateau of northern Iran (Lauer et al., 2017). In addition to climatic and biological studies, microstructural analyses using SEM have also been applied to distinguish different loess zones and textures in Golestan Province, highlighting the region's sedimentological complexity and importance in Quaternary research (Ghandhari et al., 2019).

Numerous studies have been conducted on the loess-paleosol sequences and modern paleosols in northern Iran, focusing on micromorphology and mineralogy (Khormali & Kehl, 2011); (Taheri et al., 2017); (Vlaminck et al., 2018), magnetic properties (Ghafarpour et al., 2016); (Valaee et al., 2016); (Vlaminck et al., 2018); (Pourmasoumi et al., 2019)) and systematic luminescence and radiocarbon dating (Kehl, 2010); (Vlaminck et al., 2016); (Lauer et al., 2017)). However, studies of biological archives that can be directly related to climatic conditions are still scarce in this region. These archives can assist in reconstructing elevation, temperature, and precipitation, and even enable paleoenvironmental reconstructions using biological evidence. Such studies can help fill informational gaps and enhance our understanding of climatic transformations.

Although many ecological indicators are rare or absent in loess, mollusk shells found in loess-paleosol sequences are a common phenomenon and can serve as powerful tools in reconstructing past climatic conditions (Rousseau & Wu, 1997). Terrestrial mollusks, which are easily identifiable in Quaternary sediments, act as reliable indicators for quantifying environmental conditions. They have been extensively studied in various regions worldwide to accurately estimate past climatic parameters (Moine et al., 2002). Recent studies have emphasized the importance of mollusks as paleoclimate proxies in loess–paleosol sequences, including works by Hui et al. (2021), Li et al. (2022), and Jia et al. (2024), which demonstrate the potential of malacological data for high-resolution climate reconstruction in Eurasian contexts. In Iran, however, studies utilizing biological archives directly linked to climatic conditions are rare. By employing these archives, it is possible to reconstruct elevation, temperature, and precipitation, and to recreate paleoenvironmental conditions using biological evidence. Temperature and humidity are the primary limiting factors affecting the physiology and life cycle of terrestrial mollusks. Each species has a thermal range that governs its activity (Moine et al., 2002). The response time of malacofauna to environmental changes, especially the disappearance of biomes, is less than 50 years. Mollusk shells are well-preserved in Quaternary sediments and can be identified at the species level based on their shape and ornamentation. Fossil mollusks possess carbonate shells that preserve them in various terrestrial sediments. Furthermore, they strongly reflect ecological conditions and are highly sensitive even to minor environmental changes. Consequently, they have been widely used as environmental proxies in Quaternary research over the past decades (Limondin-Lozouet et al., 2017).

Numerous studies have been conducted in Europe to reconstruct past climates using mollusks (Zong et al., 2020; Charó, 2021; Santagati, 2022; Dong et al., 2022; Quiroz-Barroso et al., 2024). Land snails collected from loess profiles have been evaluated for paleoenvironmental reconstruction. These studies involve identifying the species present in loess to map different biotopes. The distribution of species has been correlated with meteorological parameters, enabling the description of temperature gradients and mean annual temperatures. Richter et al. (2020) utilized fossil mollusk records to reconstruct environmental and climatic conditions associated with glacial-interglacial cycles up to 400,000 years ago. They demonstrated that land snails serve as valuable proxies for reconstructing past environmental conditions.

Despite valuable studies conducted in Iran on gastropods, their potential as proxies for environmental and climatic reconstruction remains underexplored. While research has addressed the biodiversity and distribution of gastropods, particularly in regions like northern Iran, their application for paleoenvironmental reconstructions is still limited (Gholinezhad et al., 2022; Hosseini et al., 2023). Given that such studies have not been conducted in Iran thus far, the primary objective of this paper is to identify fossil species in the study area during the Quaternary period in northeastern Iran, introduce new species, and document their occurrences and extinctions over different time intervals. This study aims to examine how variations in terrestrial mollusk assemblages within the loess–paleosol sequence of northern Iran reflect environmental and climatic oscillations. We hypothesize that these faunal shifts correspond to glacial–interglacial cycles and can be utilized as biological indicators for reconstructing Quaternary paleoclimates.

2. Materials and Methods:

2.1. Geography and Climate

The Sa'dabad-3 area is located at 36°49'03" North latitude and 54°22'54" East longitude, near the village of Saadabad, adjacent to the city of Gorgan in Golestan Province. Due to its geographical features, Golestan Province is influenced by factors such as elevation, distance from the sea, the presence of the southern deserts of Turkmenistan, and the blowing of local and regional winds. These factors result in a high climatic diversity within the province. Additionally, significant and water-rich rivers flow from the heights of the Alborz Mountain range in this province, including the Atrak, Gorganrud, and Gharesu rivers (Fig.1).

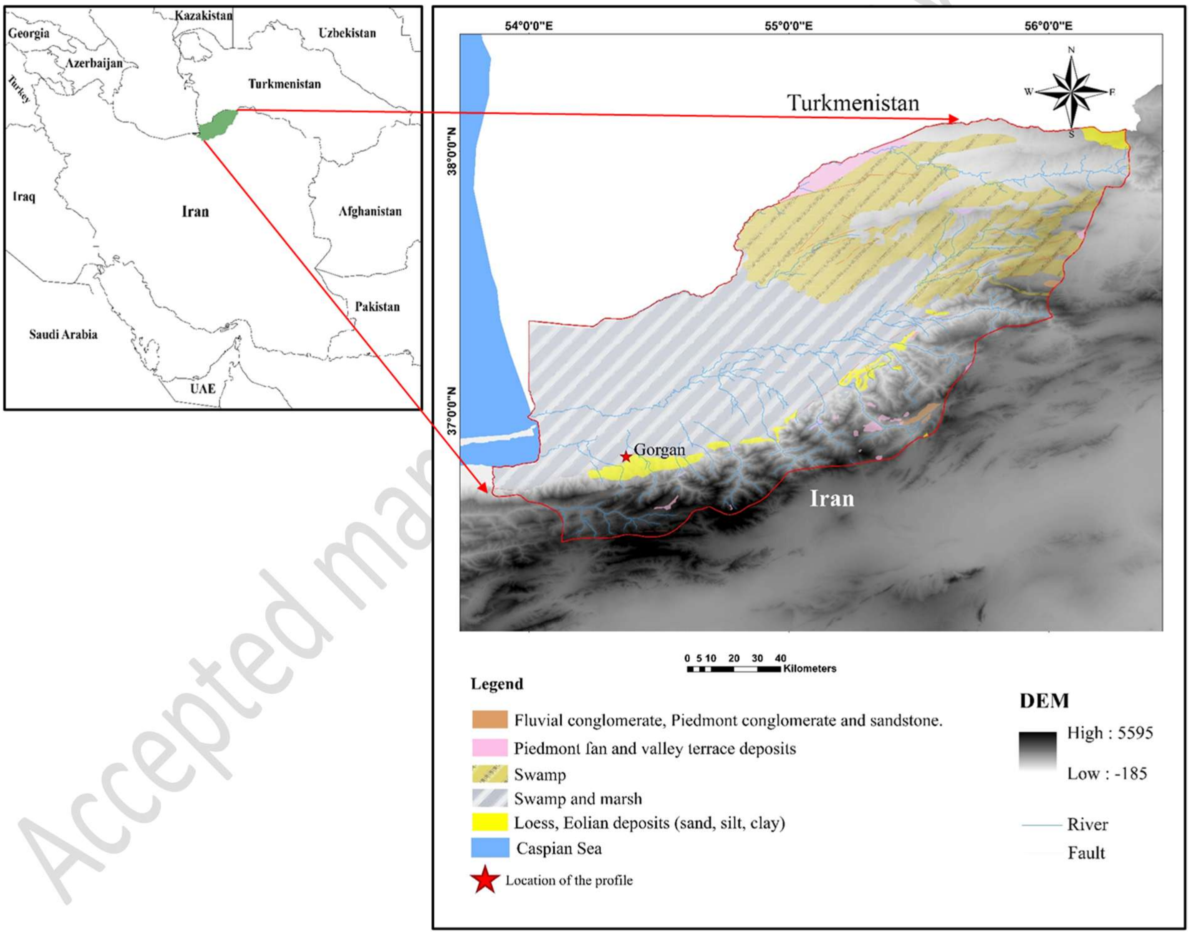

Figure 1. The location sampling station of Sa'dabad village is in the east of Golestan province.

In determining the climate of this region, two main air masses play a pivotal role. One is the cold northern air mass that enters from Siberia, bringing snowfall in the southern highlands and rain in the temperate belt during autumn and winter. The other is the western air mass originating from the Atlantic Ocean and the Mediterranean Sea, which brings precipitation in winter and increases humidity and sultry conditions in summer. Therefore, the highest rainfall occurs in winter, and the lowest in summer. In the northern half of the province, which is a dry and semi-arid region, rainfall decreases, and due to high evaporation, saline and low-yield lands are formed.

The vegetation cover of Golestan Province is diverse due to its geographical location and climatic conditions, encompassing dense forests, grasslands, and steppe regions. Proximity to the Caspian Sea and the Alborz Mountain range has led to the formation of rich vegetation from sea level to high peaks. This vegetation has developed in distinct bands from the Caspian Sea coastline up to the lofty summits.

2.2. Field Studies and Sampling

After identifying the sequence under study, preparation for sampling began (Fig. 2a). To access fresh soil surfaces, the face of the sequence was scraped using an excavator. To reach older layers and increase the sampling thickness, approximately 3 meters were excavated below ground level. Additionally, scaffolding was used to facilitate accurate and easy sampling of sections that were high and inaccessible. Before commencing the main sampling, the sequence was described and examined based on the initially collected samples. Different soil horizons were identified, and a preliminary stratigraphic column was prepared for initial studies. Sampling was carried out at 10-centimeter intervals, resulting in a total of 230 samples, each weighing 15 kilograms, collected for the examination of terrestrial mollusk shells (malacology). After sampling and completing field operations, the samples were transferred to the laboratory for preparation and subsequent procedures (Fig. 2-b, 2-c, 2-d).

In the lab, the samples underwent sieving using a 35-mesh sieve (0.5 mm) and were prepared for further steps, including the picking and identification of fossils, utilizing the wet washing method (Fig. 2- b & c). The extracted shells were then identified and counted with a stereomicroscope (Wild model M8) with a magnification of 20 to 40 times (Fig. 2-d), following the protocol outlined by Richter et al (2019).

Figure 2. Steps of sampling (a), preparation (b), isolation (c), and study of mollusks (d)

The identification of mollusk species in this study was carried out meticulously under the guidance of a malacology expert. Detailed examination of morphological features was performed using a stereomicroscope. Diagnostic characters, including shell shape and size, sculpture patterns, coiling direction (dextral or sinistral), the presence and shape of operculum, and details of the aperture, were used to ensure precise identification. Multiple authoritative taxonomic resources were consulted. Key references included Heller & Arad (2009) for terrestrial mollusks of Israel, Schileyko (2009) for species across Russia and surrounding regions, and Horsák et al. (2013) for Central European faunas. Glöer & Pešić (2012) and Mansoorian (2000) were essential in identifying and confirming freshwater species. In addition, the revisionary work by Ruud and Neubert (2016) and the recent taxonomic contributions by Mumladze et al. (2023) were consulted for Enidae.

Identification was further supported by consultation of international databases such as MolluskaBase, Catalogue of Life, and AnimalBase. Regional faunal checklists and national atlases, including "Land Snails of Iran", were also referenced to confirm species' presence and distribution within Iran.

Following species identification, all specimens were systematically counted the abundance data were then used to construct a species distribution diagram by depth to visualize changes in shell frequency along the stratigraphic profile. These diagrams were generated using Python (matplotlib library), which allowed for accurate and high-resolution visualization of faunal trends with depth. The resulting graphs formed the basis of a qualitative paleoenvironmental interpretation by highlighting fluctuations in the relative abundance of taxa. Rather than employing multivariate statistical analyses, this study adopted a descriptive approach, focusing on clear distributional patterns and their ecological implications. Interpretations were guided by species' known ecological preferences from the literature and were further supported by the pedological and stratigraphic context of the profile.

3. Results and Discussion

The profile characteristics provided detail the specific features of each soil horizon, illustrating variations in texture, structure, color, reaction to acid, presence of specific minerals, biological activities, and features such as nodules and mycelium (Fig. 3).

3.1. Litho-Malacological Description of Stratigraphic Horizons

The A horizon spans from 0 to 20 centimeters in depth. Its color is brown when dry and dark brown when wet. The texture of this horizon is silt loam, and it has a granular structure with strong to moderate angular blocks. When dry, it is very hard; when moist, it is very brittle; and when wet, it becomes sticky and plastic. The reaction to acid is slightly effervescent, and it contains numerous very fine pores and many fine roots. The counted shells in this horizon number 18, including, in order of abundance, the species *Geminula ghilanensis*, *Parmacella ibera*, *Helicella derbentina*, *Geminula didymodus*, and *Pomatias rivulare*.

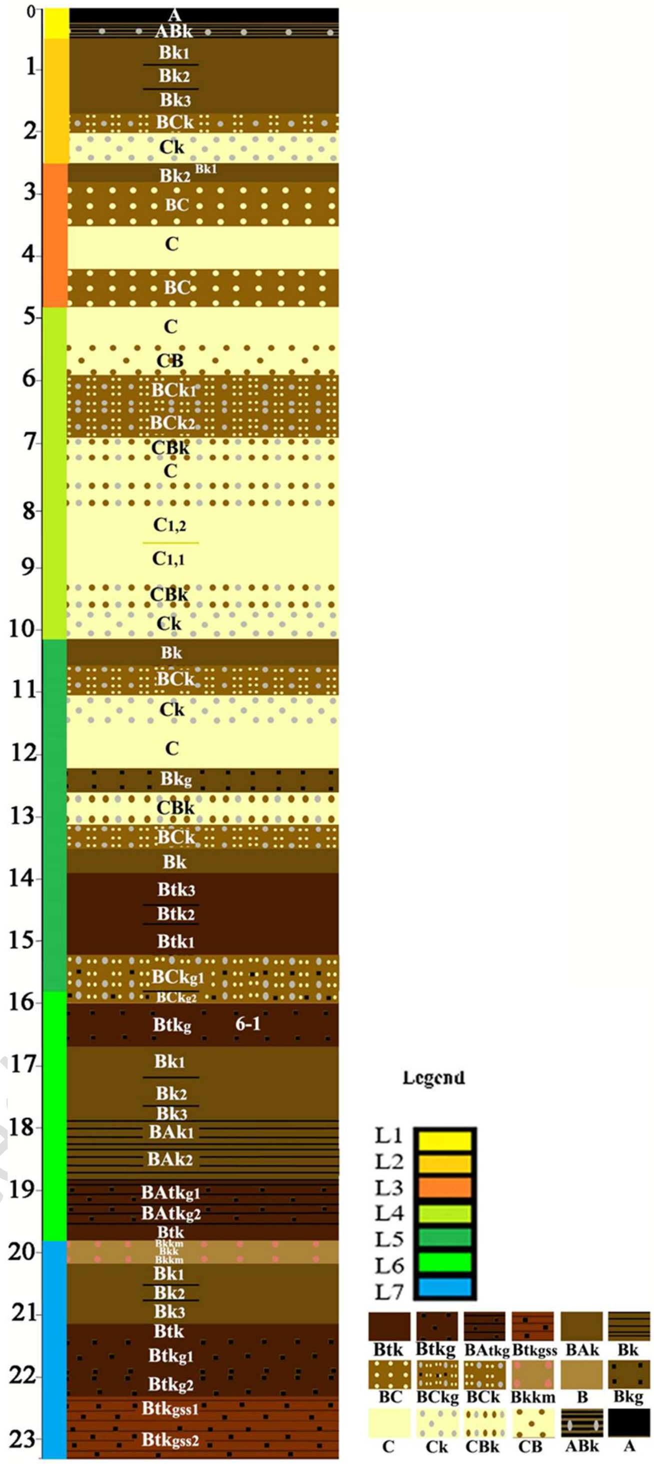

Figure 3. Loess-soil sequence at the Sa'dabad-3 showing thick layers of primary loess and moderately to strongly developed paleosol horizons.

The ABk horizon is located between 20 and 45 centimeters deep. Its color is dark yellowish-brown when dry and slightly darker when moist. The texture is also silt loam, and the structure comprises moderate to strong angular blocks. This horizon is very hard when dry, brittle when moist, and sticky and plastic when wet. It reacts strongly with acid, indicative of high carbonate content. A few pores and fine roots are observed, along with traces of biological activity such as biogenic channels. The counted shells in this horizon number 14, including, in order of abundance, the species *Geminula ghilanensis*, *Parmacella ibera*, and *Euomphalia pisciformis*. The Bk_1 horizon extends from 45 to 90 centimeters in depth. Its color is yellowish-brown when dry and slightly darker when moist. The texture is silt loam, with a moderate angular blocky structure. The reaction to acid is strongly effervescent. There are few pores and a low number of fine roots in this layer. The counted shells total 10, including the species *Euomphalia pisciformis* and *Geminula didymodus*.

The Bk_2 horizon covers depths from 90 to 130 centimeters. Its color is yellowish-brown when dry and darker yellowish-brown when moist. The texture remains silt loam, and the structure is medium angular blocky. This horizon is hard when dry, brittle when moist, and sticky and plastic when wet. It reacts strongly with acid, and fungal networks are abundantly present. The counted shells in this horizon number 8, including, in order of abundance, the species *Parmacella ibera*, *Euomphalia pisciformis*, *Geminula didymodus*, and *Cecilioides acicula*.

The Bk_3 horizon lies between 130 and 170 centimeters deep. Its color is similar to horizons Bk_1 and Bk_2, yellowish-brown when dry and darker yellowish-brown when moist. The texture is silt loam with a weak fine angular blocky structure. This horizon is slightly hard when dry, brittle when moist, and slightly sticky and plastic when wet. It reacts strongly with acid, and medium to large fungal networks are observed. The counted shells total 13, including, in order, the species *Euomphalia pisciformis*, *Geminula didymodus*, and *Buliminus halpensis*.

The BCk horizon encompasses depths from 170 to 200 centimeters. Its color is yellowish-brown when dry and darker when moist. The texture is silt loam, and the structure is massive with weak fine angular blocks. Strong effervescence occurs upon reaction with acid. A few fine pores, root channels, and abundant fungal networks are present. The counted shells in this horizon number 22, including the species *Geminula ghilanensis*, *Euomphalia pisciformis*, *Buliminus halpensis*, and *Cochlicella conoidea*.

The Ck horizon is found between 200 and 250 centimeters deep. Its color mirrors the BCk horizon, yellowish-brown when dry and darker when moist. The texture is silt loam with a massive structure. This horizon is very soft or slightly hard when dry and brittle when moist. It reacts strongly with acid, and few concentrations are observed. The counted shells total 101, including, in order of abundance, the species *Geminula ghilanensis*, *Parmacella ibera*, *Euomphalia pisciformis*, *Geminula didymodus*, *Buliminus halpensis*, and *Cochlicella conoidea*.

The Bk_1 horizon at depths 250 to 260 centimeters has a yellowish-brown color when dry and dark yellowish-brown when moist. The texture is silt loam with a weak structure of small angular blocks. It reacts strongly with acid and contains small to medium concentrations, soft masses, and a small amount of mycelium. The counted shells number 45, including, in order of abundance, the species *Euomphalia pisciformis*, *Geminula didymodus*, *Vallonia costata*, *Vallonia pulchella*, and *Cochlicella conoidea*.

The Bk_2 horizon continues from 260 to 310 centimeters deep. Its color is similar to Bk_1. The texture is silt loam with a weak structure of small angular blocks. It reacts strongly with acid and contains small to medium concentrations, soft masses, and a small amount of mycelium. The counted shells in this horizon number 170, including, in order of abundance, the species *Geminula ghilanensis*, *Parmacella ibera*, *Helicella derbentina*, *Euomphalia pisciformis*, *Geminula didymodus*, *Buliminus halpensis*, *Cecilioides acicula*, *Pomatias rivulare*, *Cochlicella conoidea*, and *Oxychilus alliarius*.

The BC horizon (modern) is located at depths of 310 to 350 centimeters. This horizon has a light yellowish-brown color when dry and a dark yellowish-brown color when moist. The texture is silty loam, and it possesses a weak structure with small angular blocks. This horizon is lime-free and exhibits no effervescence upon reaction with acid. A total of 157 shells were found in this horizon. In order of abundance, the species include *Parmacella ibera*, *Helicella derbentina*, *Euomphalia pisciformis*, *Buliminus halpensis*, *Zootecus insularis*, *Pagodulina pagodula*, and *Cecilioides acicula*.

The C horizon begins at a depth of 350 to 420 centimeters. Its color is light yellowish-brown when dry and yellowish-brown when moist. This horizon has a loess texture with a massive structure and shows no effervescence. A total of 134 shells were identified in this horizon. The species, listed in order, are *Helicella derbentina*, *Euomphalia pisciformis*, *Geminula didymodus*, *Zootecus insularis*, *Cecilioides acicula*, and *Cochlicella conoidea*.

The BC horizon extends from 420 to 480 centimeters. It displays a light yellowish-brown color when dry and a dark yellowish-brown color when moist. The texture is silty loam with a weak structure composed of small angular blocks. This horizon is lime-free and shows no effervescence upon acid reaction. A total of 143 shells were found here, including, in order of abundance, *Geminula ghilanensis*, *Parmacella ibera*, *Euomphalia pisciformis*, *Geminula didymodus*, *Zootecus insularis*, *Truncatellina collicratis*, and *Cochlicella conoidea*.

From 480 to 540 centimeters, the C horizon continues. The color remains light yellowish-brown when dry and yellowish-brown when moist. This horizon is characterized by a loess texture and a massive structure, with no reaction to acid. A total of 195 shells were collected, including the species *Geminula ghilanensis*, *Parmacella ibera*, *Euomphalia pisciformis*, *Geminula didymodus*, *Zootecus insularis*, *Truncatellina callicratis*, *Pagodulina pagodula*, *Cochlicella conoidea*, and *Oxychilus alliarius*. Additionally, 8 unidentified shells were gathered from this horizon; their identification and study are ongoing.

The CB horizon is located at depths of 540 to 590 centimeters. Its color is yellowish-brown when dry and darker yellowish-brown when moist. The structure is massive, and no effervescence is observed upon acid reaction. This horizon lacks significant pedogenic concentrations and contains a small number of shells. A total of 195 shells were found, including *Geminula ghilanensis*, *Euomphalia pisciformis*, *Geminula didymodus*, *Zootecus insularis*, *Pagodulina pagodula*, and *Cochlicella conoidea*. One unidentified shell was also collected, which is currently under investigation.

Spanning depths from 590 to 640 centimeters, the BCk_2 horizon displays a yellowish-brown color when dry and a dark yellowish-brown when moist. Its texture is silt loam with a massive structure and weak, fine, angular blocks. The horizon is hard when dry and brittle when moist. It reacts slightly with acid (weak effervescence) and contains a small number of fine micelles. A total of 247 shells were recorded, including *Geminula ghilanensis*, *Parmacella ibera*, *Euomphalia pisciformis*, *Geminula didymodus*, *Zootecus insularis*, *Truncatellina collicratis*, *Pagodulina pagodula*, and *Cochlicella conoidea*.

The BCk_1 horizon extends from 640 to 690 centimeters. It has a yellowish-brown color when dry and a dark yellowish-brown color when moist. The texture is silt loam with a massive structure and weak, fine, angular sub-blocks. The horizon is hard when dry and brittle when moist. It reacts slightly with acid and contains a small number of fine micelles and fine minerals. 227 shells were found, including *Parmacella ibera*, *Euomphalia pisciformis*, *Geminula didymodus*, *Buliminus halpensis*, *Cecilioides acicula*, *Caspicyclotus sieversi*, *Cochlicella conoidea*, and *Pseudamnicola raddei*.

Occupying depths from 690 to 730 centimeters, the CBk horizon is yellowish-brown when dry and dark yellowish-brown when moist. The texture is silt loam with a massive structure and weak, fine angular sub-blocks. It is hard when dry and brittle when moist. This horizon shows slight effervescence with acid and contains a small number of fine micelles and shell remnants. A total of 127 shells were identified, including *Euomphalia pisciformis*, *Geminula didymodus*, *Cochlicella conoidea*, and *Oxychilus alliarius*.

The C horizon is found between 730 and 760 centimeters. Its color is light yellowish-brown when dry and yellowish-brown when moist. This horizon is loess with a massive structure and does not react with acid, indicating the absence of calcareous minerals. 145 shells were collected, including *Geminula ghilanensis*, *Helicella derbentina*, *Euomphalia pisciformis*, *Geminula didymodus*, *Pagodulina pagodula*, *Pagodulina subdola*, *Cecilioides acicula*, *Cochlicella conoidea*, *Oxychilus alliarius*, *Pseudamnicola raddei*, and *Carychium lederi*. Additionally, one unidentified shell was collected and is currently being studied.

Between 760 and 800 centimeters lies the CBk horizon. It has a light yellowish-brown color when dry and yellowish-brown when moist. The texture is silt loam with a massive structure and weak, fine, angular sub-blocks. This horizon is hard when dry and brittle when moist, reacting slightly with acid and containing a small number of fine micelles. 106 shells were found here, including *Helicella derbentina*, *Euomphalia pisciformis*, *Geminula didymodus*, *Pagodulina pagodula*, *Pagodulina subdola*, *Cecilioides acicula*, *Vallonia pulchella*, *Cochlicella conoidea*, *Oxychilus alliarius*, and *Pseudamnicola raddei*.

The $C_{1,2}$ horizon spans depths from 800 to 860 centimeters. It is light yellowish-brown when dry and yellowish-brown when moist. This horizon is loess with a massive structure and shows no reaction to acid. A total of 429 shells were collected, including *Geminula ghilanensis*, *Parmacella ibera*, *Helicella derbentina*, *Euomphalia pisciformis*, *Geminula didymodus*, *Zootecus insularis*, *Pagodulina pagodula*, *Pagodulina subdola*, *Bithynia tentaculata*, *Cochlicella conoidea*, and *Lymnaea gedrosiana*. One unidentified shell was also collected and is under examination.

Extending from 860 to 920 centimeters, the $C_{1,1}$ horizon has a very pale brown color when dry and yellowish-brown when moist. This horizon is loess with a massive structure and does not react with acid. A significant number of 2,071 shells were found, including *Geminula ghilanensis*, *Parmacella ibera*, *Euomphalia pisciformis*, *Geminula didymodus*, *Truncatellina collicratis*, *Pagodulina pagodula*, *Pagodulina subdola*, *Cecilioides acicula*, *Planorbis carinatus*, *Planorbis*

planorbis, *Cochlicella conoidea*, *Lymnaea gedrosiana*, *Lymnaea truncatula*, *Gyraulus euphraticus*, *Gyraulus convexiusculus*, *Vertigo antivertigo*, *Physella acuta*, and *Valvata piscinalis*.

The CBk horizon occupies depths from 920 to 964 centimeters. It is very pale brown when dry and yellowish-brown when moist. The texture is silt loam with a massive structure and weak, fine, angular sub-blocks. This horizon is hard when dry and brittle when moist, reacting slightly with acid and containing a small number of fine micelles. A total of 1,336 shells were identified, including *Geminula ghilanensis*, *Parmacella ibera*, *Euomphalia pisciformis*, *Geminula didymodus*, *Zootecus insularis*, *Truncatellina callicratis*, *Pagodulina pagodula*, *Pagodulina subdola*, *Acicula persica*, *Pomatias rivulare*, *Caspicyclotus sieversi*, *Cochlicella conoidea*, *Oxychilus alliarius*, *Carychium lederi*, and *Granopupa persica*. Additionally, 41 unidentified shells were collected from this horizon, and their identification and study are ongoing.

The Ck horizon spans depths from 964 to 1,014 centimeters. Its color is light yellowish-brown when dry and yellowish-brown when moist. The texture is silt loam with a massive structure. This horizon is soft when dry and brittle when moist. It reacts strongly with acid and contains a small number of fine micelles. A total of 1,961 shells were found in this horizon. The species identified, in order of abundance, are: *Geminula ghilanensis*, *Parmacella ibera*, *Euomphalia pisciformis*, *Geminula didymodus*, *Zootecus insularis*, *Pagodulina pagodula*, *Pagodulina subdola*, *Vallonia costata*, *Vallonia pulchella*, *Acicula persica*, *Pomatias rivulare*, *Caspicyclotus sieversi*, *Cochlicella conoidea*, *Oxychilus alliarius*, *Vertigo pygmaea*, *Vertigo angustior*, *Granopupa persica*. Additionally, 271 unidentified shells were collected from this horizon; their identification and study are ongoing.

The Bk horizon (MIS5-1) extends from 1,014 to 1,054 centimeters. It exhibits a yellowish-brown color when dry and a dark yellowish-brown color when moist. The texture is silt loam with fine to medium subangular blocky structure. This horizon is hard when dry and brittle when moist. It reacts strongly with acid and contains numerous micelles and soft masses. A total of 404 shells were found, including: *Parmacella ibera, Euomphalia pisciformis*, *Geminula didymodus*, *Pagodulina pagodula*, *Pagodulina subdola*, *Acicula persica*, *Pomatias rivulare*, *Caspicyclotus sieversi*, *Cochlicella conoidea*, *Oxychilus alliarius.*

The BCk horizon covers depths from 1,054 to 1,104 centimeters. Its color is light yellowish-brown when dry and dark yellowish-brown when moist. The texture is silt loam with a weak fine angular blocky structure. This horizon is hard when dry and brittle when moist. It reacts slightly with acid, exhibiting weak effervescence, and contains numerous fine micelles. A total of 767 shells were found, including: *Parmacella ibera, Euomphalia pisciformis*, *Geminula didymodus*, *Cochlicella conoidea.*

The Ck horizon spans depths from 1,104 to 1,150 centimeters. It has a yellowish-brown color when dry and a dark yellowish-brown color when moist. The texture is silt loam with a massive structure and weak fine angular blocks. This horizon reacts strongly with acid. A total of 463 shells were collected, including: *Parmacella ibera*, *Euomphalia pisciformis*, *Geminula didymodus*, *Pagodulina pagodula*, *Cochlicella conoidea*, *Oxychilus alliarius*. Additionally, one unidentified shell was gathered from this horizon, which is currently under study.

The C horizon extends from 1,150 to 1,220 centimeters. Its color is light yellowish-brown when dry and yellowish-brown when moist. The texture is silt loam with a massive structure. This horizon does not react with acid. A total of 1,961 shells were found, including: *Geminula ghilanensis*, *Euomphalia pisciformis*, *Geminula didymodus*, *Zootecus insularis*, *Vallonia pulchella*, *Cochlicella conoidea*, *Oxychilus alliarius*, *Granopupa persica.*

The Bkg horizon (MIS5-2) covers depths from 1,220 to 1,260 centimeters. It appears brown when dry and dark brown when moist. The texture is silt loam with fine to medium angular blocky structure. This horizon is hard when dry and brittle when moist. It reacts slightly with acid and contains numerous fine micelles. A total of 52 shells were identified, including: *Euomphalia pisciformis, Geminula didymodus, Pagodulina subdola, Cochlicella conoidea.*

The CBk horizon is located at depths of 1,260 to 1,310 centimeters. The soil is light brown when dry and yellowish-brown when moist. It is composed of silt loam with a massive structure and fine subangular blocks. This horizon reacts strongly with acid and typically contains mycelial networks. A total of 442 shells were collected, including: *Geminula ghilanensis, Parmacella ibera*, *Euomphalia pisciformis*, *Geminula didymodus*, *Pagodulina pagodula*, *Pagodulina subdola*, *Vallonia costata*, *Vallonia pulchella*, *Pomatias rivulare*, *Cochlicella conoidea*, *Oxychilus alliarius*, *Granopupa persica.* Additionally, 26 unidentified shells were gathered from this horizon; their identification and study are ongoing.

At depths of 1,310 to 1,350 centimeters, the BCk horizon shares a similar color to the previous horizon. It is also composed of silt loam but is characterized by a structure with weak angular blocks and a strong reaction to acid. Carbonate minerals, soft masses, and small sand grains are observed. Fine mycelium, iron/manganese oxides (Fe/Mn), and various terrestrial snails are present. A total of 1,354 shells were found, including: *Geminula ghilanensis*, *Parmacella ibera*, *Euomphalia pisciformis*, *Geminula didymodus*, *Zootecus insularis*, *Pagodulina pagodula*, *Pagodulina subdola*, *Vallonia costata*, *Vallonia pulchella*, *Acicula persica*, *Pomatias rivulare*, *Caspicyclotus sieversi*, *Cochlicella conoidea*, *Oxychilus alliarius*, *Granopupa persica.* Additionally, 231 unidentified shells were collected from this horizon, which are currently being identified and studied.

In the Bk horizon at depths of 1,350–1,390 millimeters, the soil color changes to light brown when dry and brown when moist. This horizon is a silt loam with a structure of weak medium subangular blocks. It exhibits a strong reaction with acid. Carbonate minerals, mycelial masses, and medium mineral particles are commonly found in this horizon. A total of 273 shells were collected here, including, in order of abundance: *Parmacella ibera*, *Euomphalia pisciformis*, *Geminula didymodus*, *Vallonia costata*, *Vallonia pulchella*, *Acicula persica*, *Pomatias rivulare*, *Cochlicella conoidea*, *Oxychilus alliarius*, *Granopupa persica*. Additionally, 111 unidentified shells were gathered from this horizon; their identification and study are ongoing.

The Btk_3 horizon at depths of 1,390–1,440 millimeters is reddish-brown when dry and reddish-brown when moist. This horizon is silty clay with a massive and hard structure when dry. It shows a weak to moderate reaction with acid and is characterized by the presence of clay skins and observable mycelium. No shells were found in this horizon.

In the Btk_2 horizon between 1,440 and 1,470 millimeters, the soil color shifts to brown when dry and dark brown when moist. This horizon is also silty clay with a medium angular blocky structure that is hard when dry. It reacts strongly with acid. No shells were found in this horizon.

The Btk_1 horizon (MIS 5e) at depths of 1,470–1,520 millimeters has soil that is brown when dry and dark brown when moist. This soil is silty clay with a medium, angular, blocky, and hard structure when dry. It shares characteristics with the previous horizon, except that it does not exhibit a strong reaction with acid. The presence of iron/manganese oxides and clay skins is widespread. No shells were found in this horizon.

At depths of 1,520–1,580 millimeters, the CBkk horizon is light brown when dry and yellowish-brown when moist. This horizon is silt loam with a structure of weak subangular blocks and shows a strong reaction with acid. Iron/manganese oxides, fine mycelia, and soft masses are present. A total of 458 shells were identified, including: *Parmacella ibera*, *Euomphalia pisciformis*, *Geminula didymodus*, *Zootecus insularis*, *Pagodulina pagodula*, *Pomatias rivulare*, *Caspicyclotus sieversi*, *Cochlicella conoidea*, *Oxychilus alliarius*, *Granopupa persica*

The BCkg horizon (MIS 5e) is located at depths of 1,580–1,600 millimeters and is yellowish-brown when dry and dark brown when moist. This soil is silt loam with a weak angular blocky structure and reacts strongly with acid. Iron/manganese oxides and fine mycelia are commonly observed. A total of 86 shells were found, including: *Parmacella ibera*, *Zootecus insularis*, *Vallonia pulchella*, *Acicula persica*, *Pomatias rivulare*, *Caspicyclotus sieversi*, *Granopupa persica.*

In the Btkg horizon (Paleo I) at depths of 1,600–1,670 millimeters, the soil is yellowish-brown when dry and dark brown when moist. This soil is silt loam to silty clay loam with a medium angular blocky structure and reacts strongly with acid. The presence of iron/manganese oxides and soft masses is noted. A total of 92 shells were collected, including: *Euomphalia pisciformis*, *Geminula didymodus*, *Pomatias rivulare*, *Granopupa persica.*

At depths of 1,670–1,720 millimeters, the Bk_1 horizon is light yellowish-brown when dry and dark brown when moist. This soil is silt loam with a medium angular blocky structure and reacts strongly with acid. 70 shells were found, including: *Geminula ghilanensis*, *Parmacella ibera*, *Euomphalia pisciformis*, *Geminula didymodus*, *Granopupa persica*

The Bk_2 horizon from 1,720 to 1,763 millimeters has a similar color to the previous horizon and is also silt loam. This horizon reacts strongly with acid and contains soft masses and medium mineral bodies. 24 shells were identified, including: *Geminula ghilanensis*, *Euomphalia pisciformis*, *Geminula didymodus.*

Between 1,763 and 1,786 millimeters, the Bk_3 horizon is pale brown when dry and yellowish-brown when moist. This soil is silt loam with a medium angular blocky structure and reacts strongly with acid. 11 shells were found, including: *Geminula ghilanensis*, *Parmacella ibera*, *Euomphalia pisciformis*, *Oxychilus alliarius.*

In the BAk_1 horizon (Paleo II) at depths of 1,786–1,825 millimeters, the soil is light brown when dry and dark yellowish-brown when moist. This horizon is silt loam with a medium angular blocky structure and reacts strongly with acid. Mycelia and soft masses are observed. Only 4 shells were collected, including: *Parmacella ibera*, *Zootecus insularis.* Additionally, 2 unidentified shells were gathered from this horizon; their identification and study are ongoing.

The BAk_2 horizon from 1,825 to 1,882 millimeters has a yellowish-brown color when dry and dark brown when moist. This soil ranges from silty clay loam to silt loam and reacts strongly with acid. Fine mycelia and soft masses are commonly present. A total of 188 shells were found, including: *Parmacella ibera*, *Euomphalia pisciformis*, *Geminula didymodus*, *Zootecus insularis*, *Acicula persica*, *Pomatias rivulare*, *Caspicyclotus sieversi*, *Cochlicella conoidea*, *Granopupa persica.*

At depths of 1,882–1,922 millimeters, the $BAtkg_1$ horizon (Paleo III) is yellowish-brown when dry and dark brown when moist. This soil is silty clay with a medium angular blocky structure and reacts strongly with acid. The presence of mycelia and soft masses is another characteristic of this horizon. No shells were found in this horizon.

The $BAtkg_2$ horizon between 1,922 and 1,970 millimeters has a yellowish-brown color when dry and dark brown when moist. This soil is silty clay with a medium to fine angular blocky structure and reacts strongly with acid. Soft masses, mycelia, and iron/manganese oxides are prominent features. No shells were found in this horizon.

The Btk horizon spans depths from 1,970 to 2,000 millimeters. Its color is yellowish-brown when dry and dark yellowish-brown when moist. The texture ranges from silt loam to silty clay loam, with a weak fine angular blocky structure. This horizon exhibits a weak to non-reactive response to acid and contains fine minerals, clay skins, and iron/manganese oxides within pores. 42 shells were collected, including: *Geminula ghilanensis*, *Parmacella ibera*, *Euomphalia pisciformis*, *Pomatias rivulare*, *Caspicyclotus sieversi.*

The Bkkm horizon spans depths from 2,000 to 2,010 centimeters. Its color is brownish-yellow when dry and yellowish-brown when moist. This horizon is petrocalcic, with portions partially cemented. It reacts strongly with acid and contains several shells. A total of 133 shells were found in this horizon, including, in order of abundance, the species: *Parmacella ibera*, *Pagodulina pagodula*, *Pomatias rivulare*, *Caspicyclotus sieversi*, *Cochlicella conoidea*, *Oxychilus alliarius*, *Granopupa persica.*

The Bkk horizon occupies depths from 2,010 to 2,023 centimeters. Its color is brownish-yellow when dry and yellowish-brown when moist. The texture is silty loam with a weak, fine subangular blocky structure. This horizon reacts strongly with acid and includes long calcitic concretions measuring 2–3 centimeters. A total of 32 shells were found in this horizon, including, in order of abundance, the species: *Euomphalia pisciformis*, *Pagodulina subdola*, *Caspicyclotus sieversi.*

The Bkkm horizon extends from 2,023 to 2,034 centimeters. Its color is brownish-yellow when dry and yellowish-brown when moist. This horizon is petrocalcic, with parts partially cemented. It reacts strongly with acid. Only 2 shells were found in this horizon, both belonging to the species *Caspicyclotus sieversi*.

The Bk_1 horizon (paleosol) occupies depths from 2,034 to 2,070 centimeters. Its color is pale brownish-yellow when dry and brownish-yellow when moist. The texture is silty loam with a weak, fine, angular blocky structure. This horizon reacts strongly with acid and contains numerous soft masses and fungal micelles. Common concretions are typically observed in this horizon. Only one shell of the species *Caspicyclotus sieversi* was identified in this horizon.

The Bk_2 horizon spans depths from 2,070 to 2,095 centimeters. Its color is brownish-yellow when dry and dark brownish-yellow when moist. The texture is silty loam with a weak, fine subangular blocky structure. This horizon reacts strongly with acid and commonly contains fungal micelles and soft masses. A total of 9 shells were found, including: *Parmacella ibera*, *Euomphalia pisciformis.*

The Bk_3 horizon covers depths from 2,095 to 2,133 centimeters. Its color is brownish-yellow when dry and dark brownish-yellow when moist. The texture is silty loam with fine to medium subangular blocky structure. This horizon reacts strongly with acid and includes fungal micelles, soft masses, and concretions. No shells were found in this horizon.

The Btk horizon (paleosol) extends from 2,133 to 2,159 centimeters. Its color is light brown when dry and brown when moist. The texture is silty loam with fine to medium angular blocky structure. This horizon reacts strongly with acid and includes long calcitic structures up to 5 centimeters, iron/manganese oxides, and fungal micelles. No shells were found in this horizon.

The $Btkg_1$ horizon covers depths from 2,159 to 2,212 centimeters. Its color is brownish to dark brown when dry and brown when moist. The texture is silty loam with medium angular blocky structure. This horizon is weakly reactive to non-reactive with acid and contains clay skins, iron/manganese oxides, and calcitic structures. No shells were found in this horizon.

The $Btkg_2$ horizon spans depths from 2,212 to 2,250 centimeters. Its color is pale brownish-yellow when dry and brownish-yellow when moist. The texture is silty loam with medium angular blocky structure. This horizon is weakly reactive to non-reactive with acid and includes iron/manganese oxides and fine calcitic minerals. No shells were found in this horizon.

The $Btkgss_1$ horizon (PS6) extends from 2,250 to 2,290 centimeters. Its color is pale brown when dry and brown when moist. This horizon has a silty loam texture with medium to strong angular blocky structure. It is weakly reactive to non-reactive with acid and includes iron/manganese oxides, slickensides, and long calcitic nodules. No shells were found in this horizon.

The $Btkgss_2$ horizon occupies depths from 2,290 to 2,350 centimeters. Its color is brown when dry and dark brown when moist. The texture is silty loam with medium to coarse angular blocky structure. This horizon is weakly reactive to non-reactive with acid and contains soft masses, long calcitic structures, and slickensides. Features such as slickensides and shiny surfaces are observed in this horizon.

3.2. Introduction of New Species in the Sa'dabad-3 Sequence

The following species have been identified as new fossils in Golestan Province:

Planorbis carinatus (Müller, 1774), *Gyraulus euphraticus* (Mousson, 1874), *Gyraulus convexiusculus* (Hutton, 1849), *Geminula ghilanensis* (Issel, 1865), *Geminula didymodus* (O. Boettger, 1880), *Helicella derbentina* (Krynicki, 1836), *Zootecus insularis* (Ehrenberg, 1831), *Oxychilus alliarius* (Miller, 1822), *Pseudamnicola raddei* (Boettger, 1889), *Helicopsis persica* (Hausdorf & Bössneck, 2016), *Truncatellina callicratis* (Scacchi, 1833), *Cecilioides acicula* (Müller, 1774), *Pupilla muscorum* (Linnaeus, 1758), *Pupilla triplicata* (Studer, 1820), *Cochlicella conoidea* (Draparnaud, 1801), *Granopupa persica* (Gittenberger, 1973)

1. *Planorbis carinatus* (Müller, 1774)

This species possesses a shell similar in size to *Planorbis planorbis*, but features 4 to 5 whorls. The shell has a prominent keel in the center of the body whorl. *Planorbis carinatus* is considered an aquatic species. It is reported here for the first time in Golestan Province, observed at a depth of 910 centimeters in the study area. Overall, only 8 shells of this species were recorded throughout the section (Fig. 4, 1a, b).

2. *Gyraulus euphraticus* (Mousson, 1874)

This species has a relatively broad shell without significant grooves and a smooth surface lacking cross-striation. The shell diameter rarely reaches 8 millimeters, with a height less than 1.5 millimeters. It comprises between 3.5 and a maximum of 4.5 whorls, with the last and largest whorl showing a slight deviation. Compared to the genus *Planorbis*, the genus *Gyraulus* has a much smaller shell, though they closely resemble each other in appearance. This species is newly reported for Golestan Province, with only one shell collected at a depth of 870 centimeters (Fig. 4, 2a, b).

3. *Gyraulus convexiusculus* (Hutton, 1849)

This species features a small, thin, flattened, white, and semi-transparent shell with an ovate aperture. Its whorls do not increase in diameter as rapidly as those of *Gyraulus costulatus*. In the initial whorls, there is a slight angle near the center, and the last whorl is almost uniformly curved. A relatively coarse spiral pattern is observable in most specimens (Wright, 1963; Brown and Wright, 1980). The diameter and height of adult shells are approximately 5 millimeters and 1.2 millimeters, respectively. This freshwater species is newly reported for Golestan Province, with only one shell collected from a depth of 870 centimeters (Fig. 4, 3a, b).

4. *Geminula ghilanensis* (Issel, 1865)

This species has an egg-shaped shell with an open, slit-like umbilicus. It possesses between 6.8 to 9.1 whorls that are relatively convex with deep sutures. The teleoconch exhibits irregular oblique striations without any spiral grooves. The shell is relatively sturdy, semi-transparent, and horn-yellow in color, with a white stripe behind the peristome. The aperture is thickened by a labial callus, and the columellar and palatal connections are visibly joined by the callus. There is no basal lamella present. The shells of this very small snail are about 3 millimeters in height and have a barrel or vase shape, with a slightly ear-shaped open aperture. This species is newly reported for Golestan Province and was observed at nearly all depths in our study area, with a total of 172 specimens collected (Fig. 4, 4a, b).

5. *Geminula didymodus* (O. Boettger, 1880)

This species has a right-handed shell, approximately cylindrical to egg-shaped, with an open, slit-like umbilicus. It has between 6.1 to 8.0 whorls that are relatively convex with deep sutures. The shell is relatively sturdy, semi-transparent, and horn-yellow in color with a white stripe behind the peristome. The aperture is thickened by a labial callus. A distinguishing feature is a tooth on the basal margin of the aperture, which is absent in *G. ghilanensis* and serves as the main differentiator between the two species. This species is newly reported for Golestan Province and was observed at almost all depths in our study area, with 677 specimens collected (Fig. 4, 5a, b).

6. *Helicella derbentina* (Krynicki, 1836)

This species has a low-conical shell with a round spire whose height sometimes does not exceed that of the peristome. The shell surface exhibits fine transverse striae, and occasionally, rare weak spiral lines. It is white, monochrome, and less commonly with lines or rows of spots, usually displaying two rows of spots. This snail has 5 to 5.5 convex whorls that increase rapidly and uniformly in size. The embryonic whorls are smooth and dark. The aperture edges are sharp, thin, and simple. The umbilicus is wide but not fully exposed. Shell size ranges between 8 to 12 millimeters in height and 15 to 20 millimeters in width. This species is newly reported for Golestan Province and was collected at depths of 10 centimeters, 380 centimeters, 850 centimeters, and 1,330 centimeters, totaling 81 specimens (Fig. 4, 6a, b).

7. *Zootecus insularis* (Ehrenberg, 1831)

This species features a white, thick shell with widely spaced apical whorls forming a conical shape. The aperture is quasi-rectangular with a thickened peristome. The umbilicus is open, though it may sometimes be nearly covered by the reflected columellar edge of the peristome. Shell size ranges between 11–15 millimeters in length and 3.5–6 millimeters in width. This species is newly reported for Golestan Province and was observed at most depths in our study area, with 82 specimens collected (Fig. 4, 7a, b).

8. *Oxychilus alliarius* (Miller, 1822)

This species has a low cylindrical shell with a wide spire, where the height is approximately equivalent to that of the peristome. The shell is covered with weak, indistinct transverse striations, is nearly smooth, and has very fine spiral lines. It is highly glossy and transparent, with a pale yellow to dark brown color and a white surrounding the umbilicus. The shell has 4 to 5 prominent whorls that initially increase slowly and then more rapidly. The umbilicus is funnel-shaped and prominent. Shell height ranges from 3 to 3.5 millimeters, and width from 6 to 7 millimeters. This species is newly reported for Golestan Province and was observed at various depths in our study area, with 24 specimens collected in this sequence (Fig. 4, 8a, b).

9. *Pseudamnicola raddei* (Boettger, 1889)

This species has a white, conical shell with 4.5 whorls, each distinctly separated by a clear suture. The shell surface is glossy and features fine striations. The apex is blunt, and the umbilicus is closed. The aperture is oval, with a pointed top. Shell height ranges from 2.4 to 2.6 millimeters, and its width is approximately 1.9 millimeters. Distinctive characteristics include the conical shell with a pointed aperture. This species is newly reported for Golestan Province, with 24 specimens collected at depths of 760 centimeters, 1,350 centimeters, and 1,600 centimeters (Fig. 4, 9a, b).

10. *Helicopsis persica* (Hausdorf & Bössneck, 2016)

This species has a discoidal or sunken-conical shell featuring 4.5 to 5 highly prominent whorls. The shell is white adorned with yellow-brown stripes or color zones. The aperture is lemon-shaped, and the upper insertion of the peristome is either not inclined or only slightly inclined toward the aperture. The umbilicus is slightly eccentric, encompassing approximately 14 to 18% of the shell's diameter. Shell diameter ranges from 9.3 to 12.2 millimeters (mean 10.6 ± 0.8 mm), while shell height varies from 5.3 to 7.7 millimeters (mean 6.4 ± 0.6 mm). This species is newly reported for Golestan Province, with seven specimens collected at depths of 1,840 centimeters and 1,870 centimeters in our study area (Fig. 4, 10a, b).

11. *Truncatellina callicratis* (Scacchi, 1833)

This species features a cylindrical shell with fine, uniform striations and a light straw-yellow color. It has 5 to 6 whorls. The peristome is triangular to rounded, with reflected edges and a small lip. Three teeth are present within the aperture. The umbilicus appears slit-like. The shell dimensions range from 1.5 to 1.8 millimeters in height and 0.75 to 0.8 millimeters in width. The height and width of the peristome measure between 0.45 and 0.55 millimeters. This snail is newly reported for Golestan Province and was observed at various depths in the study areas, with a total of 104 specimens collected (Fig. 4, 11a, b).

12. *Cecilioides acicula* (Müller, 1774)

The shell is elongated, very slender, glossy, and smooth with a blunt apex. In juvenile specimens, the shell is transparent with a pale-yellow color. After the snail's death, the shell becomes opaque and white. This species has 5 to 6 slightly swollen whorls that increase slowly in width and slightly faster in height. The whorls are separated by a narrow, oblique suture. The height of the final whorl is slightly more than half the total shell height. The peristome is narrow with a sharp angle at the top. The height of the peristome is slightly more than one-third of the shell's height. The outer edge of the peristome descends almost vertically and protrudes slightly forward in the middle. The shell height ranges from 4.5 to 5 millimeters, and the width from 1 to 1.3 millimeters. Most species of this genus live deep in the soil and are usually blind. This snail is newly reported for Golestan Province and was observed at almost all depths in our study area, with a total of 19 specimens collected (Fig. 4, 12a, b).

13. *Pupilla muscorum* (Linnaeus, 1758)

This snail has an oval, cylindrical shell. The shell is usually light brown, varying from reddish-brown to horn-gray, and is slightly striated or nearly smooth. It has 5 to 6.5 weakly convex whorls with not very deep sutures. The aperture typically features a well-developed lip, a clear constriction on the upper edge, and no teeth are observed within. Shell height ranges from 3 to 4 millimeters, and width from 1.65 to 1.75 millimeters (the shell diameter varies little). This species is newly reported for Golestan Province and was collected at a depth of 1,030 centimeters in our study area (Fig. 4, 13a, b).

14. *Pupilla triplicata* (Studer, 1820)

The shell of this snail is smaller than those of other *Pupilla* species and has a finer surface structure. It possesses 6 convex whorls. Typically, there are three teeth in the aperture: one on the roof, one on the left side, and another on the lower part of the aperture. Shell height ranges from 2.2 to 2.8 millimeters (up to 4 millimeters), and shell width is about 1.4 millimeters. This species is newly reported for Golestan Province and was collected only once at a depth of 1,020 centimeters in our study area (Fig. 4, 14a, b).

15. *Cochlicella conoidea* (Draparnaud, 1801)

This snail's shell has 5 or 6 whorls. Its apex is blunt or rounded, and there is an umbilical opening near the aperture. This species is newly reported for Golestan Province and was collected in our study area at depths of 180–1,370 centimeters, 1,540–1,580 centimeters, and 1,840–1,870 centimeters, with a total of 1,943 specimens collected (Fig. 4, 15a, b).

16. *Granopupa persica* (Gittenberger, 1973)

This species is newly reported for Golestan Province and was collected at depths of 940–1,010 centimeters, 1,300–1,360 centimeters, 1,540–1,610 centimeters, 1,720 centimeters, 1,840 centimeters, and 2,010 centimeters in our study area. A total of 581 specimens of this snail were collected (Fig. 4, 16a, b).

3.3. Stratigraphic Subdivision of the Sa'dabad-3 Loess Profile

The Sa'dabad-3 loess–paleosol sequence, located near Gorgan in northeastern Iran, was examined in detail through field-based stratigraphic and pedological analysis (Fadavi et al. 2024). Observations of soil horizons, including their color, structure, texture, carbonate morphology, and other morphological features, were used to construct the stratigraphic column and interpret the depositional history of the profile.

Since absolute dating techniques (e.g., luminescence or radiocarbon dating) were not available, the profile was subdivided based on a combination of direct field observations and stratigraphic correlation with nearby loess sections, specifically the well-studied profiles at Agh Band and Nodeh. These neighboring sections, which are situated within the same geomorphological and climatic context, have been previously investigated and partially dated (e.g., Khormali & Kehl, 2011; Frechen et al., 2009), providing a suitable regional reference for relative dating.

By comparing the main loess and paleosol layers, carbonate accumulations, and degree of soil development observed in the Sa'dabad-3 section with those in the Agh Band and Nodeh profiles, the Sa'dabad-3 sequence was divided into seven major stratigraphic zones (. These zones reflect alternating phases of loess deposition and soil formation associated with Quaternary climatic changes. The following sections of the manuscript provide a detailed description of each zone and its paleoenvironmental significance.

3.4. Malacological Zonation and Age Correlation

The Sa'dabad-3 profile, approximately 23 meters thick, encompasses seven loess-paleosol sequences labeled from top (P1 and L1) to bottom (P7 and L7) as illustrated in Figure 4. Based on these sequences, we have delineated seven zones for malacological study in this area. Similar loess-soil sequences at the Neka, Now Deh, and Agh Band sections exhibit thick layers of primary loess and developed paleosol horizons (Khormali & Kehl, 2011). By comparing our loess sequence with those from Neka, Now Deh, and Agh Band, where dating studies have been conducted, we estimate the approximate age of the Sa'dabad-3 sequence at a depth of 23 meters to be around 300,000 years.

Zone 1 corresponds to the late Holocene interglacial period and extends from the surface to a depth of approximately 50 cm. This surface layer contains several terrestrial mollusk species, including Helicella derbentina, Geminula didymodus, Geminula gilanensis, Euomphalia pisciformis, Drusia ibera, and Pomatias rivulare. In total, 36 shells were identified, accounting for only 0.28% of all samples (Fig. 5). Despite the warm and humid climate of this interglacial interval, the fossil abundance is unexpectedly low. This may be due to the short duration of sediment accumulation and the intense pedogenic activity in Holocene soils. In such conditions, calcium carbonate in shells dissolves rapidly due to rainfall and organic matter, leading to poor fossil preservation. The disappearance of Pomatias rivulare in the next zone and the gradual increase in species richness and abundance toward Zone 2 reflect environmental changes over time (Machette, 1985).

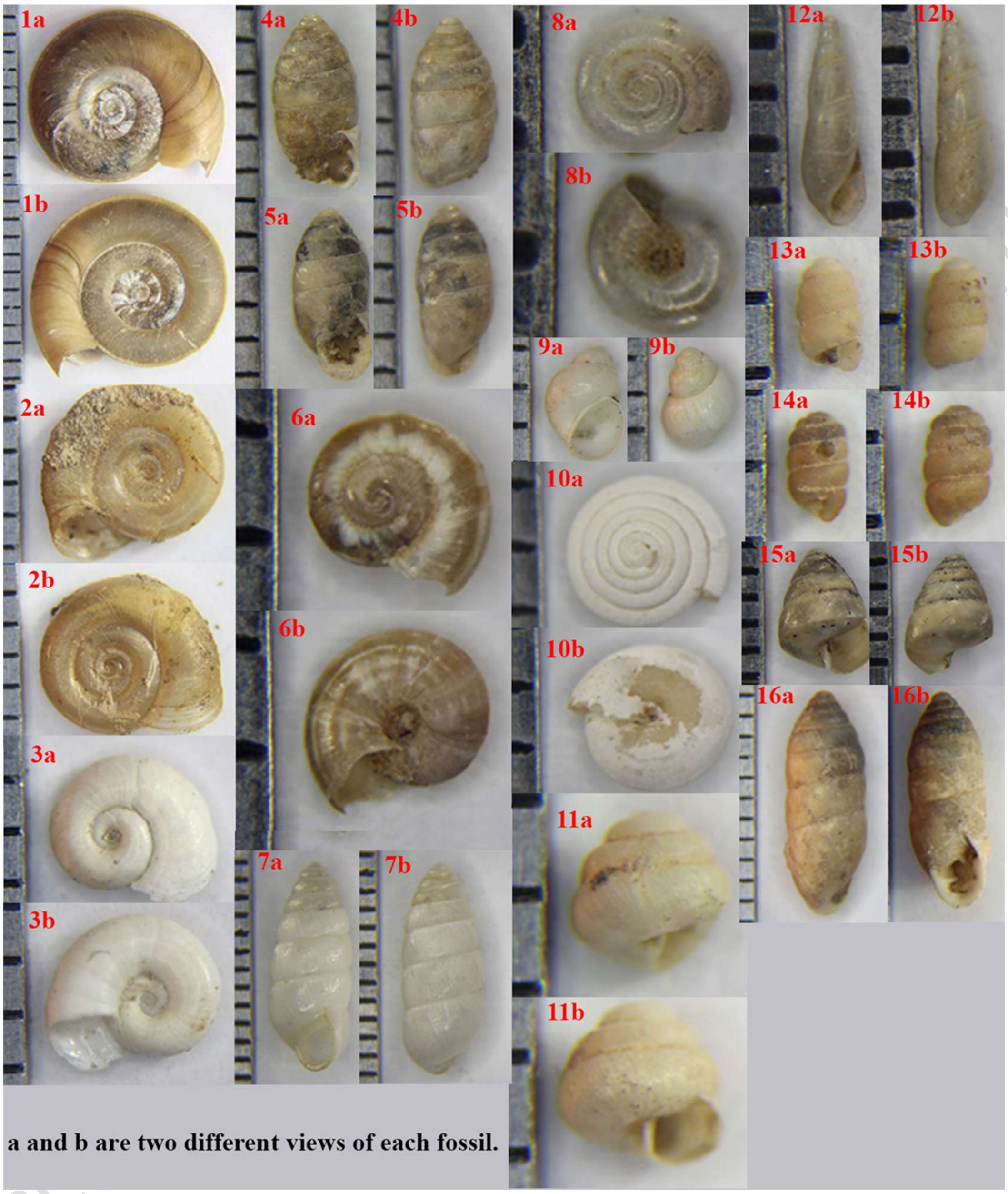

Figure 4. Fossils found in different loess-paleosol layers of the Sa'dabad3. 1a,b. *Planorbis carinatus,* 2a,b. *Gyraulus euphraticus*, 3a,b. *Gyraulus convexiusculus,* 4a,b. *Geminula ghilanensis,* 5a,b. *Geminula didymodus,* 6a,b. *Helicella derbentina* 7a,b. *Zootecus insularis,* 8a,b. *Oxychilus alliarius,* 9a,b. *Pseudamnicola raddei,* 10a,b. *Helicopsis persica,* 11a,b. *Truncatellina callicratis,* 12a,b. *Cecilioides acicula,* 13a,b. *Pupilla muscorum,* 14a,b. *Pupilla triplicate,* 15a,b. *Cochlicella conoidea,* 16a,b. *Granopupa persica*

Zone 2 corresponds to a previous interglacial period, possibly Marine Isotope Stage (MIS) 5, and extends from 50 to 260 cm below the surface. This layer contains a more diverse mollusk assemblage compared to Zone 1, including Helicella derbentina, Geminula didymodus, Geminula gilanensis, Euomphalia pisciformis, Drusia ibera, Buliminus halpensis, Cecilioides acicula, Cochlicella conoidea, and Oxychilus alliarius. A total of 150 shells were recovered, marking a noticeable increase in both abundance and species richness with the addition of several new taxa. These changes suggest relatively warm and stable environmental conditions typical of interglacial periods. However, the overall fossil abundance remains modest (1.16% of total samples, Fig. 5), which may be due to strong pedogenic processes and carbonate leaching under humid soil conditions. Such factors likely contributed to the limited preservation of calcareous remains, despite favorable ecological conditions for mollusk habitation (Zamanian, 2016).

Zone 3 likely represents a transitional phase between interglacial and glacial periods and extends from 260 to 490 cm in depth. This zone contains a diverse assemblage of mollusks, including Helicella derbentina, Geminula didymodus, Geminula gilanensis, Euomphalia pisciformis, Drusia ibera, Zootecus insularis, Truncatellina callicratis, Pagodulina pagodula, Vallonia costata, Vallonia pulchella, Pomatias rivulare, Cochlicella conoidea, and Oxychilus alliarius. A total of 649 shells were recorded, accounting for 5.03% of all samples (Fig. 5), a fivefold increase in comparison to the preceding zone. While this interval may be expected to reflect cooling conditions, the elevated abundance and richness of mollusks suggest the influence of intermittent warm or humid episodes. It has been shown that moisture availability plays a more significant role than temperature in determining gastropod abundance (Brown, 1994). Furthermore, the loessic nature of the sediments in this zone may have promoted rapid burial and limited soil formation, enhancing fossil preservation. These factors together indicate relatively favorable environmental conditions during this transitional phase (Antoine et al., 2001).

Zone 4 extending from 490 to 1,110 cm, represents a full glacial period and remarkably contains the highest mollusk shell abundance and species diversity in the entire sequence. A total of 7,962 shells were identified, comprising 61.67% of all samples (Fig. 5). In addition to species observed in earlier zones, this interval includes numerous new taxa such as Pagodulina subdola, Bithynia tentaculata, Planorbis carinatus, Planorbis planorbis, Lymnaea gedrosiana, Lymnaea truncatula, Gyraulus euphraticus, Gyraulus convexiusculus, Vertigo antivertigo, Vertigo pygmaea, Vertigo angustior, Physella acuta, Valvata piscinalis, Pseudamnicola raddei, Carychium lederi, Granopupa persica, Pupilla muscorum, and Laciniaria lederi. The presence of freshwater species such as Bithynia, Planorbis, and Lymnaea points to the existence of shallow ponds or temporary wetlands during this glacial interval. These microhabitats, together with rapid burial in carbonate-rich loess and minimal soil development, created favorable conditions for fossil preservation. Despite the cold climatic setting, the ecological richness indicates that the local environment sustained a surprisingly complex and diverse malacofauna (Moine et al., 2002).

Zone 5 corresponds to an older interglacial period characterized by relatively warm and stable climatic conditions. This interval yielded approximately 3,630 mollusk shells, accounting for 28.12% of all samples (Fig. 5), making it the second-most abundant zone after Zone 4. The species diversity in this layer is comparable to that of the previous zone, suggesting ecological stability and a well-developed malacofauna. However, the number of shells is roughly half that of the glacial Zone 4, which is counterintuitive given the interglacial context. This reduction in fossil abundance may result from decreased preservation potential in organic-rich, acidic soils typical of forested environments. Under such conditions, elevated moisture and biological activity can enhance carbonate dissolution. Furthermore, while species richness remained high, actual snail population densities may have been lower in densely vegetated ecosystems. These factors collectively help explain the discrepancy between ecological conditions and fossil abundance in this zone (Bailey et al., 2005).

Zone 6 Zone 6 represents a transitional phase from an interglacial to a glacial period and extends from 1,700 to 2,100 cm. The fossil assemblage includes species similar to those recorded in previous zones; however, the total abundance declines markedly, with only 483 identifiable mollusk shells (3.74% of the total (Fig. 5)). This notable reduction aligns with a shift toward cooler and drier climatic conditions, typical of the early stages of glaciation. The decreasing abundance likely reflects environmental changes that reduced habitat suitability for gastropods, such as declining vegetation cover, soil moisture, and temperature. The data from this zone indicate a gradual ecological deterioration consistent with the onset of a glacial regime (Moine et al., 2002).

Zone 7, the deepest and final section of the profile, spans from 2,100 to 2,330 cm and is entirely devoid of mollusk remains. This complete absence indicates extremely unfavorable conditions for gastropod life and fossilization. The zone is attributed to a severe glacial period, likely corresponding to Marine Isotope Stage (MIS) 8, approximately 300,000 years ago. The extreme cold or prolonged aridity during this time may have led to the collapse of suitable habitats for snails. Alternatively, the sedimentary context, possibly dominated by coarse alluvial materials, may have been unsuitable for mollusk colonization or for preserving their shells. Regardless of the exact cause, the fossil void in Zone 7 aligns with paleoenvironmental expectations for a highly inhospitable glacial interval (Radaković et al., 2024).

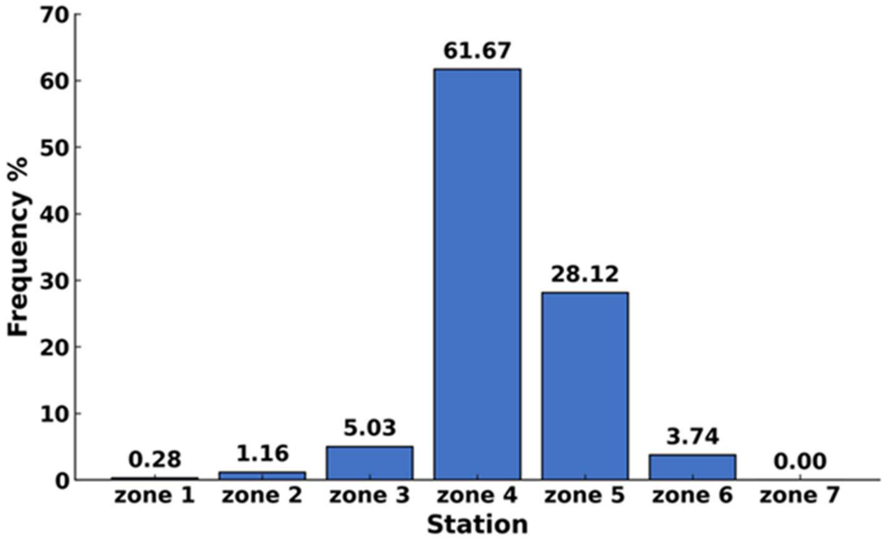

Figure 5. Frequency percentage of mollusks in the studied stations

3.5. Ecoclimatic Interpretation of Mollusk Abundance by Depth

The following figure illustrates the abundance of the top 10 most common mollusk species identified in the Sa'dabad-3 profile, plotted against depth. This data provides insights into paleoenvironmental shifts across seven stratigraphic zones from the late Holocene to the Middle Pleistocene (Fig. 6).

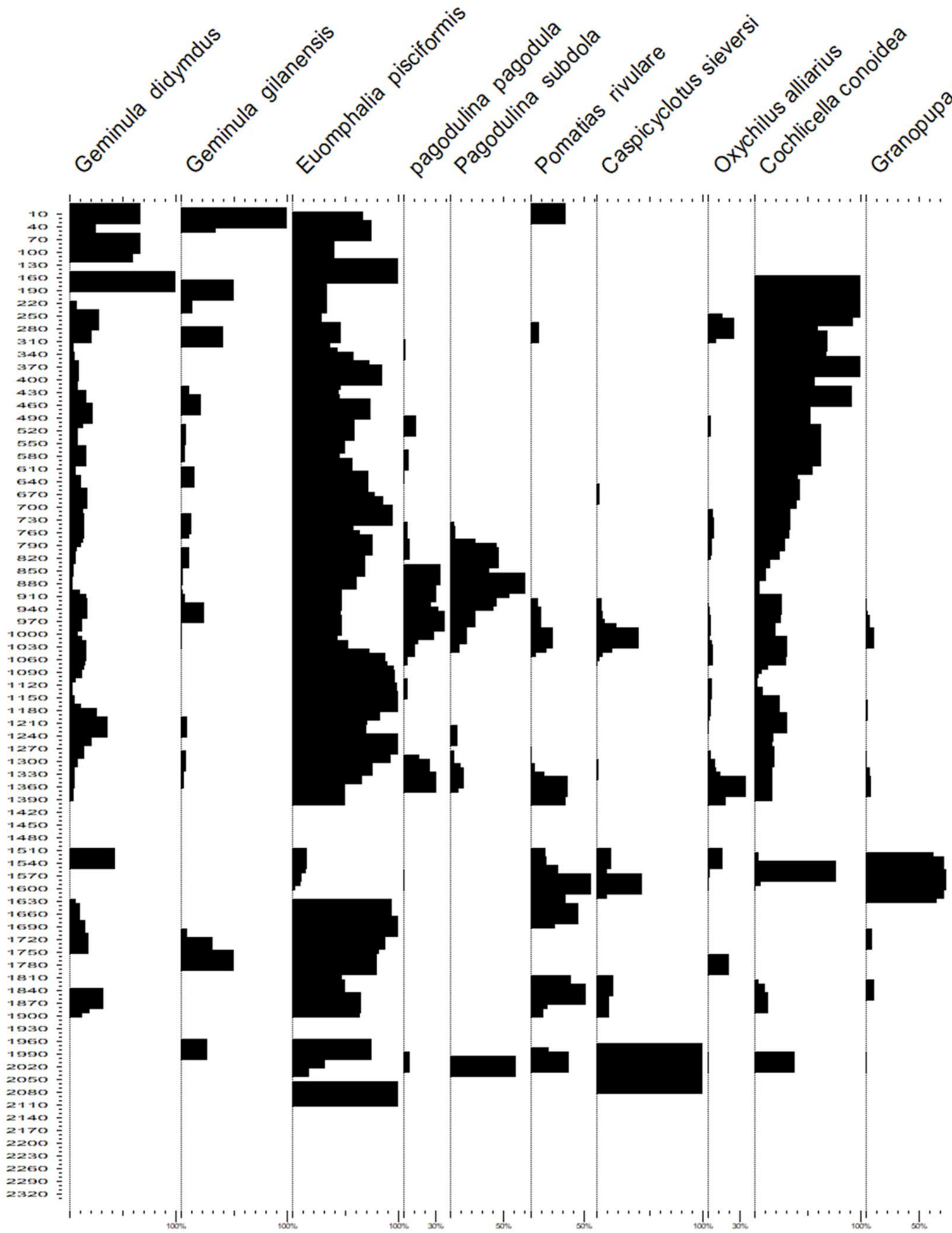

Figure 6. Mollusk species identified in the Sa'dabad-3 profile, plotted against depth.

The species abundance trends show clear ecological transitions. Zone 1 (0–50 cm) presents minimal mollusk presence, suggesting recent pedogenic activity and dissolution. Zone 2 (50–260 cm), although interglacial, reflects moderate diversity but low abundance. In contrast, Zone 3 (260–490 cm) shows an increase in abundance, likely due to favorable humidity and loess sedimentation. Zone 4 (490–1110 cm), assigned to a glacial period, shows the highest abundance and diversity, attributed to preservation in carbonate-rich loess and the presence of shallow aquatic habitats. Zone 5 (1110–1700 cm), an older interglacial, maintains high diversity but lower preservation due to acidic organic soils. Zone 6 (1700–2100 cm) marks a decline in abundance with cooling trends, and Zone 7 (2100–2330 cm) lacks fossils entirely, corresponding to harsh glacial conditions.

Although loess layers are generally associated with glacial periods and expected to contain fewer land snail shells due to harsh, cold-dry conditions, and paleosols with interglacial, more favorable warm-humid climates and richer assemblages, this expected pattern was not consistently observed in the Sa'dabad-3 profile. For instance, Zone 4, which corresponds to a loess horizon, exhibited unexpectedly high species richness and abundance. In contrast, some paleosol layers, such as those in Zone 5, showed relatively low total shell counts despite stable species diversity.

Such deviations from the typical glacial–interglacial model have also been documented in other loess–paleosol sequences around the world. For example, Rousseau & Wu (1997) reported anomalous mollusk assemblages in the Luochuan loess section in China, which they attributed to short-term climatic oscillations not recorded in the soil development. Similar results have been reported by Wu & Wu (2011), who found higher shell concentrations in certain loess units (e.g., L9LL2) compared to neighboring paleosols in the Chinese Loess Plateau. They attributed this to favorable preservation conditions in loess, including rapid burial and alkaline environments, which reduce shell dissolution.

These findings reinforce the idea that shell abundance should be interpreted within a broader taphonomic and sedimentological context, not solely as a direct climatic signal. Similarly, Moine et al. (2002) observed unexpected increases in species diversity within loess horizons in northern France, suggesting that localized microclimatic effects and ecological niches may have played a role. Moreover, Ložek (1965) emphasized that taphonomic processes, preservation conditions, and even human or animal activity could significantly influence fossil mollusk abundances.

These findings highlight the importance of integrating ecological, stratigraphic, and sedimentological evidence when interpreting paleoenvironmental signals from mollusk data. In the case of the Sa'dabad-3 section, the observed inconsistencies likely reflect the complex interaction between climate, local soil moisture, microhabitat variability, and preservation conditions rather than large-scale climatic anomalies.

4. Conclusion

A comprehensive analysis of mollusk species discovered in the Sa'dabad-3 loess stratigraphy in Gorgan, Iran, has introduced 16 new species to the region's malacofauna. By examining 12,910 mollusk specimens from 230 samples, the study identified 37 species spanning 28 genera and 25 families, underscoring the rich biodiversity preserved in the loess-paleosol sequences. The delineation of seven distinct zones within the profile, each reflecting glacial and interglacial periods, provides valuable insights into past climatic conditions. Clear patterns of mollusk distribution and abundance across glacial-interglacial stages emphasize their potential as sensitive indicators of past environmental changes. This correlation enhances our understanding of climate-driven terrestrial ecosystem dynamics in the Quaternary period.

These findings have broader implications for reconstructing paleoenvironments in underexplored regions such as northern Iran and highlight the role of malacological data in improving regional and global climate models.

Future research is encouraged to incorporate additional paleoenvironmental proxies such as stable isotopes, magnetic susceptibility, and palynological records to complement mollusk-based interpretations and achieve a more robust, multi-proxy reconstruction of past climate variations. Geochemical analyses and weathering indices should also be considered to enhance the environmental interpretation of loess-paleosol sequences.

Author contributions

F. F., M. A., S. M., and F. K. designed the study, F. F., S. M., and F. K. conducted the field campaign, and collected all the sample material. F. F. and S. M. wrote the manuscript; all the authors contributed to the discussion and interpretation of the data. F. F. and E. A. conducted the mollusk analysis.

Data availability

All the data from this study are permanently stored and available online at www.pangaea.de and www.ncei.noaa.gov

Declaration of competing interest

The authors declare no competing interests.

Acknowledgments

This study was funded by the Iranian National Science Foundation (INSF) through project No. 99006758. We thank Reza Shahbazi and Morteza Sheikh from the GSI for supporting the preparation of samples. We are grateful to the editor Rahim Dabiri and Abdollah Yazdi, and two anonymous referees for their thoughtful comments.

Referencec

Antoine, P., Rousseau, D.-D., Zöller, L., Lang, A., Munaut, A.-V., Hatté, C., & Fontugne, M. (2001). High-resolution record of the last Interglacial–glacial cycle in the Nussloch loess-palaeosol sequences, Upper Rhine Area, Germany. *Quaternary International, 76*, 211-229. DOI: https://doi.org/10.1016/S1040-6182(00)00104-X

Bailey, J. V., Cohen, A. S., & Kring, D. A. (2005). Lacustrine fossil preservation in acidic environments: implications of experimental and field studies for the Cretaceous–Paleogene boundary acid rain trauma. *Palaios, 20*(4), 376-389. DOI: https://doi.org/10.2110/palo.2003.p03-88

Brown, D. S. (1994). Freshwater snails of Africa and their medical importance: *CRC Press*.

Charó, M. (2021). Quaternary marine Mollusk Associations of the last interglacials in North patagonia (Argentina): paleoecology and paleoclimates. In *Update on Malacology*: IntechOpen. DOI: https://doi.org/10.1201/9781482295184

Chenari, A. D., Feiznia, S., Aleali, M., & Ghorashi, M. (2025). Geochemistry of core sediments in the southern coast of Caspian Sea, Mazandaran, Iran: Implication for paleoclimate. *Iranian Journal of Earth Sciences*. DOI: https://doi.org/10.57647/j.ijes.2025.16794

Dong, J., Yan, H., Zong, X., Wang, G., Liu, C., Xing, M., . . . An, Z. (2022). Ultra-high resolution δ18O of land snail shell: A potential tool to reconstruct frequency and intensity of paleoprecipitation events. *Geochimica et Cosmochimica Acta, 327*, 21-33. DOI: https://doi.org/10.1016/j.gca.2022.04.015

Fadavi, F and Ahmadi, E and Khormali, F and Akbari, M and Maleki, S (2024) Land snail shell abundance in the loess-paleosol sequence of Saadabad 3, (Gorgan),*3rd International Conference and 6th National Conference of Quaternary Sciences* - Quaternary Society of Iran,Tehran.

Frechen, M., Kehl, M., Rolf, C., Sarvati, R., & Skowronek, A. (2009). Loess chronology of the Caspian lowland in northern Iran. *Quaternary International, 198*(1-2), 220-233. DOI: https://doi.org/10.1016/j.quaint.2008.12.012

Ghafarpour, A., Khormali, F., Balsam, W., Karimi, A., & Ayoubi, S. (2016). Climatic interpretation of loess-paleosol sequences at Mobarakabad and Aghband, Northern Iran. *Quaternary Research, 86*(1), 95-109. DOI: https://doi.org/10.1016/j.yqres.2016.05.004

Ghandhari, S., Amini, A., Solgi, A., & Rezaei, H. (2019). Analysis of loess sediment texture in Golestan province according to the microstructure parameters. *Iranian Journal of Earth Sciences, 11*(4), 244-255. DOI: https://doi.org/10.30495/ijes.2019.669399

Gholinezhad, N., Ashja Ardalan, A., & Malek, M. (2022). Identification and distribution of Gastropods in the east coasts of Qeshm Island (the Persian Gulf, Iran). *Iranian Journal of Fisheries Sciences, 21*(5), 1298-1315. URL: http://jifro.ir/article-1-4732-en.html

Glöer, P., & Pešić, V. (2012). The freshwater snails (Gastropoda) of Iran, with descriptions of two new genera and eight new species. *ZooKeys*(219), 11. DOI: https://doi.org/ 10.3897/zookeys.219.3406

Heller, J., & Arad, Z. (2009). *Land snails of the land of Israel: natural history and a field guide*: Pensoft. ISBN: 978-954-642-510-2

Horsák, M., Juřičková, L., & Picka, J. (2013). Mollusks of the Czech and Slovak republics. ISBN: 978- 80-86447-15-5

Hosseini, F., Siahkalroudi, S. Y., & Kheradpir, N. (2023). Species diversity of terrestrial mollusks in Shemiranat county, Tehran province with introducing four new species for Iranian fauna. *Scientific Reports in Life Sciences, 4*(1), 33-43. DOI: https://doi.org/10.5281/zenodo.7633988

Hui, Z., Ran, M., Li, H., Liu, C., Guo, B., Zhang, J., . . . Pan, Y. (2021). Early Pleistocene pollen record from the western Chinese Loess Plateau and its implications for the evolution of the East Asian Summer Monsoon. *Science of the Total Environment, 761*, 143304. DOI: https://doi.org/10.1016/j.scitotenv.2020.143304

Jia, Y.-n., Yan, H., Dong, J., Kang, S., Wang, G., Liu, C., . . . Dodson, J. (2024). Hydrothermal and eco-environmental evolution on the southeastern Chinese Loess Plateau since the last deglaciation: Evidence from terrestrial mollusk records. *Quaternary Science Reviews, 331*, 108648. DOI: https://doi.org/10.1016/j.quascirev.2024.108648

Kehl, M. (2010). Quaternary loesses, loess-like sediments, soils, and climate change in Iran. ISBN: 978-3-443-09024-1

Khormali, F., & Kehl, M. (2011). Micromorphology and development of loess-derived surface and buried soils along a precipitation gradient in Northern Iran. *Quaternary International, 234*(1-2), 109-123. DOI: https://doi.org/10.1016/j.quaint.2010.10.022

Lauer, T., Frechen, M., Vlaminck, S., Kehl, M., Lehndorff, E., Shahriari, A., & Khormali, F. (2017). Luminescence-chronology of the loess palaeosol sequence Toshan, Northern Iran–A highly resolved climate archive for the last glacial–interglacial cycle. *Quaternary International, 429*, 3-12. DOI: https://doi.org/10.1016/j.quaint.2015.03.045

Li, F., Wu, N., Zhang, D., Rousseau, D.-D., Yang, Y., Hao, Q., . . . Lu, H. (2022). Glacial-interglacial evolution of seasonal cooling events documented by land-snail eggs from Chinese loess. *Quaternary Science Reviews, 284*, 107506. DOI: https://doi.org/10.1016/j.quascirev.2022.107506

Limondin-Lozouet, N., Villa, V., Pereira, A., Nomade, S., Bahain, J.-J., Stoetzel, E., . . . Nicoud, E. (2017). Middle Pleistocene molluskan fauna from the Valle Giumentina (Abruzzo, Central Italy): Palaeoenvironmental, biostratigraphical and biogeographical implications. *Quaternary Science Reviews, 156*, 135-149. DOI: https://doi.org/10.1016/j.quascirev.2016.11.029

Liu, T., Ding, Z., & Rutter, N. (1999). Comparison of Milankovitch periods between continental loess and deep-sea records over the last 2.5 Ma. *Quaternary Science Reviews, 18*(10-11), 1205-1212. DOI: https://doi.org/10.1016/S0277-3791(98)00110-3

Ložek, V. (1965). Problems of analysis of the Quaternary nonmarine molluscan fauna in Europe.

Machette, M. N. (1985). Calcic soils of the southwestern United States. DOI: https://doi.org/10.1130/SPE203-p1

Mansoorian, A. (2000). Some freshwater snails from Northern Iran. *Iranian Journal of Public Health, 29*(1-4), 77-82. DOI: https://ijph.tums.ac.ir/index.php/ijph/article/view/1716

Moine, O., Rousseau, D.-D., Jolly, D., & Vianey-Liaud, M. (2002). Paleoclimatic reconstruction using mutual climatic range on terrestrial mollusks. *Quaternary Research, 57*(1), 162-172. DOI: https://doi.org/10.1006/qres.2001.2286

Mumladze, L., Grego, J., & Szekeres, M. (2023). The land snail family Clausiliidae (Gastropoda, Pulmonata, Stylommatophora) in Georgia: overview, novel records and a new species. *Caucasiana, 2*, 29-61. DOI: https://doi.org/10.3897/caucasiana.2.e101013

Pourmasoumi, M., Khormali, F., Ayoubi, S., Kehl, M., & Kiani, F. (2019). Development and magnetic properties of loess-derived forest soils along a precipitation gradient in northern Iran. *Journal of Mountain Science, 16*(8), 1848-1868. DOI: https://doi.org/10.1007/s11629-018-5288-4

Quiroz-Barroso, S. A., Guerrero-Arenas, R., García-Barrera, P., & Sánchez-Beristain, F. (2024). Molluska: Bivalvia and Gastropoda. In *Past Environments of Mexico: Unveiling the Past Environments of a Megadiverse Country Through its Fossil Record* (pp. 63-97): Springer. DOI: https://doi.org/10.1007/978-3-031-51034-2_4

Radaković, M. G., Gavrilović, B., Gavrilov, M. B., Marković, R. S., Hao, Q., Schaetzl, R. J., . . . Antić, A. (2024). A Glacial–Interglacial Malacofauna Record from the Titel Loess Plateau, Serbia, between~ 350 and 250 ka. *Quaternary, 7*(2), 28. DOI: https://doi.org/10.3390/quat7020028

Richter, C., Roettig, C.-B., Wolf, D., Groh, K., Kolb, T., & Faust, D. (2019). Changes in Pleistocene gastropod faunas on Fuerteventura (Canary Islands) and implications on shifting palaeoenvironmental conditions. *Quaternary Science Reviews, 209*, 63-81. DOI: https://doi.org/10.1016/j.quascirev.2019.02.005

Richter, C., Wolf, D., Walther, F., Meng, S., Sahakyan, L., Hovakimyan, H., ... & Faust, D. (2020). New insights into Southern Caucasian glacial–interglacial climate conditions inferred from Quaternary gastropod fauna. Journal of Quaternary Science, 35(5), 634-649. DOI: https://doi.org/10.1002/jqs.3204

Rousseau, D.-D., & Wu, N. (1997). A new molluskan record of the monsoon variability over the past 130 000 yr in the Luochuan loess sequence, China. *Geology, 25*(3), 275-278. DOI: https://doi.org/10.1130/0091-7613(1997)025<0275:ANMROT>2.3.CO;2

Rutter, N. W., Rokosh, D., Evans, M. E., Little, E. C., Chlachula, J., & Velichko, A. (2003). Correlation and interpretation of paleosols and loess across European Russia and Asia over the last interglacial–glacial cycle. *Quaternary Research, 60*(1), 101-109. DOI: https://doi.org/10.1016/S0033-5894(03)00069-3

Ruud, A., & NEUBERT, E. (2016). Notes on Enidae, 7. Revision of the Enidae of Iran, with special reference to the collection of Jacques de Morgan (Gastropoda: Pulmonata). DOI: https://doi.org/10.5281/zenodo.375861 10.5281/zenodo.375861

Santagati, P., Bernasconi, M. P. E., Borrelli, M., & Perri, E. (2022). Biogeographic and paleoclimatic characterization of Tyrrhenian (MIS 5e) molluskan assemblage from the Mar Piccolo of Taranto. In *Paleodays 2022 Volume dei riassunti*. DOI: https://hdl.handle.net/20.500.11770/340889

Schileyko, A. (2009). *Land snails and slugs of Russia and adjacent countries*: Pensoft publishers. ISBN: 978-954-642-474-7

Taheri, M., Khormali, F., Wang, X., Amini, A., Wei, H., Kehl, M., . . . Chen, F. (2017). Micromorphology of the lower Pleistocene loess in the Iranian Loess Plateau and its paleoclimatic implications. *Quaternary International, 429*, 31-40. DOI: https://doi.org/10.1016/j.quaint.2016.01.063

Valaee, M., Ayoubi, S., Khormali, F., Lu, S. G., & Karimzadeh, H. R. (2016). Using magnetic susceptibility to discriminate between soil moisture regimes in selected loess and loess-like soils in northern Iran. *Journal of Applied Geophysics, 127*, 23-30. DOI: https://doi.org/10.1016/j.jappgeo.2016.02.006

Vlaminck, S., Kehl, M., Lauer, T., Shahriari, A., Sharifi, J., Eckmeier, E., . . . Frechen, M. (2016). Loess-soil sequence at Toshan (Northern Iran): Insights into late Pleistocene climate change. *Quaternary International, 399*, 122-135. DOI: https://doi.org/10.1016/j.quaint.2015.04.028

Vlaminck, S., Kehl, M., Rolf, C., Franz, S. O., Lauer, T., Lehndorff, E., . . . Khormali, F. (2018). Late Pleistocene dust dynamics and pedogenesis in Southern Eurasia–Detailed insights from the loess profile Toshan (NE Iran). *Quaternary Science Reviews, 180*, 75-95. DOI: https://doi.org/10.1016/j.quascirev.2017.11.010

Wu, B., & Wu, N. (2011). Terrestrial mollusk records from Xifeng and Luochuan L9 loess strata and their implications for paleoclimatic evolution in the Chinese Loess Plateau during Marine Oxygen Isotope Stages 24-22. *Climate of the Past, 7*(2), 349-359. DOI: https://doi.org/10.5194/cp-7-349-2011

Zamanian, K., Pustovoytov, K., & Kuzyakov, Y. (2016). Pedogenic carbonates: Forms and formation processes. *Earth-Science Reviews, 157*, 1-17. DOI: https://doi.org/10.1016/j.earscirev.2016.03.003

Zong, X., Dong, J., Cheng, P., Song, Y., Liu, W., Li, Y., & Lan, J. (2020). Terrestrial mollusk records in the loess sequences from eastern Central Asia since the last deglaciation and their paleoenvironmental significance. *Palaeogeography, Palaeoclimatology, Palaeoecology, 556*, 109890. DOI: https://doi.org/10.1016/S1040-6182(00)00104-X

AnimalBase. (2024). *Biological database of animal species*. University of Göttingen. Retrieved April 10, 2025, from https://www.animalbase.uni-goettingen.de

Catalogue of Life. (2024). *Annual Checklist*. Retrieved April 10, 2025, from https://www.catalogueoflife.org

MolluskaBase. (2024). *World database of mollusk species*. Retrieved April 10, 2025, from https://www.molluskabase.org